Publications

Available Online

J. Sci. Res. **5** (1), 33-42 (2013)

JOURNAL OF SCIENTIFIC RESEARCH

www.banglajol.info/index.php/JSR

Theoretical investigation on Elastic, Thermodynamic and Optical Properties of Li_3P Ionic Conductor

M. A. Hossain[1*] and A. K. M. A. Islam[2]

[1]Physics Department, Mawlana Bhashani Science and Technology University, Santosh, Tangail-1902, Bangladesh

[2]Physics Department, Rajshahi University, Rajshahi-6205, Bangladesh

Received 26 October 2012, accepted in revised form 21 December 2012

Abstract

The elastic, thermodynamic and optical properties of Li_3P have been studied for the first time using the plane-wave ultrasoft pseudopotential technique which is based on the first-principles density functional theory (DFT) within generalized gradient approximation (GGA). The optimized lattice parameters, independent elastic constants, Young's modulus E, bulk modulus B, shear modulus G, Cauchy's pressure, Pugh's ductility index (G/B), and Poisson's ratio υ have been calculated and discussed. The temperature and pressure dependence of bulk modulus, Debye temperature, specific heats, and thermal expansion coefficient are all obtained through the quasi-harmonic Debye model with phononic effects for $T = 0-1000$ K and $P = 0-35$ GPa. The large reflectivity in the ultraviolet energy region between 7–13.4 eV indicates the material to be a good candidate as coating to avoid solar heating.

Keywords: Li_3P; *ab initio* calculations; Elastic properties; Thermodynamic properties; Optical properties.

doi: http://dx.doi.org/10.3329/jsr.v5i1.12413 J. Sci. Res. **5** (1), 33-42 (2013)

1. Introduction

Lithium phosphide has been introduced as a good ionic conductor [1]. The preparation, characterization and conductivity measurements of lithium phosphide (Li_3P) made it possible to monitor the transition from ionic to metallic conductor [2]. Li_3P crystallizes in the hexagonal A_3X (A = alkali metals; X = group 15 elements) structure with $P6_3/mmc$ space group [3-4]. The crystal structure consists of Li^+ and P^{3-} ions which are stacked in two kinds of alternating layers perpendicular to the c axis. The first layer is made up of a graphite-like Li1 and P (layer I) and the second layer is composed of a chair form cyclohexane-like Li2 (layer II). P atoms are surrounded by five Li atoms in a trigonal-

* *Corresponding author*: anwar647@gmail.com

bipyramidal arrangement. Three Li1 atoms in layer I form an equatorial triangle around P and two Li2 atoms forming layer II are axial to the Li1 triangle. The atomic positions of Li1, Li2 and P atoms in Li_3P are (0, 0, ¼), (1/3, 2/3, 0.5839) and (1/3, 2/3, ¼), respectively [5]. Solid electrolytes with high ionic conductivity are required for high energy density lithium batteries.

There is a growing need for high energy density batteries for application in microelectronic devices, power tools, and even large scale energy storage systems [6]. Advanced batteries such as, lithiated graphite/solid electrolyte/metal oxides, are very promising, nonpolluting, high energy power sources. Solid electrolytes have many advantages over liquid electrolytes in terms of design flexibility and miniaturization of the electronic devices. Solid electrolytes can be made in thin film configurations which provide a low ohmic resistance [7]. The ionic conductivity of many available solid electrolytes is too low (at ambient temperature) to be useful for high energy power sources. Commercial development of a solid state lithium battery relies on the successful development of a solid electrolyte with high ionic conductivity [8]. During last few years, the search for new ion conducting materials has focused on a series of metallate, phosphate, sulphate, silicate and borate glasses [9]. Among these materials Li_3P is one of the most important ionic conductors and it can be used for solid state lithium batteries. Nazri *et al.* [10] has used Li_3P ionic conductor during preparation of Li_3P-LiCl solid electrolyte for solid state lithium batteries.

The theoretical and experimental studies have been performed to investigate structural and electronic properties [6-8] of Li_3P. Besides the structural and electronic properties, the study of elastic, thermodynamic and optical properties of Li_3P are also important for practical applications. But there is no experimental and theoretical information on elastic, thermodynamic and optical properties of Li_3P. The knowledge of elastic constants is essential for many practical applications related to the mechanical properties of materials, e.g. load deflection, sound velocities, internal strain, thermo-elastic stress. These also offer important information regarding the degree of anisotropy which is known to correlate with a tendency to either ductility or brittleness. The microscopic thermodynamic properties are closely related to the microscopic dynamics of atoms. Thermodynamic properties of solid materials are directly related to the quanta of lattice vibrations known as phonons. Phonons directly contribute to a number of phenomena such as the thermal expansion, temperature dependence of mechanical properties, phase transitions and phase diagrams. The specific heat of a material is one of the most important thermodynamic properties indicating its heat retention or loss ability. On the other hand the optical properties of solids provide an important tool for studying energy band structure, impurity levels, excitons, localized defects, lattice vibrations, and certain magnetic excitations. The optical conductivity or the dielectric function indicates a response of a system of electrons to an applied field.

In this work, the elastic properties such as independent elastic constants, Young's modulus, ratio of the shear modulus to bulk modulus (Pugh's indicator), Cauchy's pressure, Poisson's ratio, elastic anisotropy are calculated for the first time. The

thermodynamic properties such as bulk modulus, specific heat capacities (C_P, C_V), volume thermal expansion coefficient and Debye temperature at elevated temperature and pressure are calculated and analyzed for the first time by using quasi-harmonic Debye model. The optical properties such as reflectivity, absorption, refractive index, dielectric function, conductivity and loss function are also studied for the first time using DFT within the generalized gradient approximation (GGA) method as implemented in CSATEP code at T = 0 K.

2. Theoretical methods

The present results have been obtained using CASTEP code [11] which utilizes the plane-wave pseudopotential based on density functional theory (DFT). The electronic exchange-correlation energy is treated under the generalized gradient approximation (GGA) in the scheme of Perdew-Burke-Ernzerhof (PBE) [12]. The interactions between ion and electron are represented by ultrasoft Vanderbilt-type pseudopotentials for Li, and P atoms [13]. We have got a good convergence for the total energy calculation with the choice of cutoff energy at 300 eV using the 7×7×7 *k*-point grids generated according to the Monkhorst-Pack scheme [14]. Geometry optimization is achieved using convergence thresholds of 5×10^{-6} eV/atom for the total energy, 0.01 eV/Å for the maximum force, 0.02 GPa for the maximum stress and 5×10^{-4} Å for maximum displacement. Integrations in the reciprocal space were performed by using the tetrahedron method with a *k*-mesh of 20 *k*-points in the irreducible wedge of Brillouin zone (BZ). The total energy is converged to within 0.1mRy/unit cell during the self consistency cycle.

The thermodynamic properties have been studied within the quasi-harmonic Debye model implemented in the Gibbs program [15]. The detailed description of the quasi-harmonic Debye model can be found in the literature [16-19]. Through this model, one could calculate the thermodynamic parameters including the bulk modulus, thermal expansion coefficient, specific heats, and Debye temperature etc. at any temperatures and pressures using the DFT calculated *EV* data at T = 0 K, P = 0 GPa and the Birch-Murnaghan EOS [20].

3. Results and discussion

3.1. *Structural properties*

Experimental studies have established that Li_3P crystallizes in hexagonal structure with space group $P6_3/mmc$ (194) and has 8 atoms in one unit cell. We have performed the geometry optimization as a function of the normal stress by minimizing the total energy. The calculated equilibrium lattice constants within GGA are listed in Table 1. Results from earlier experimental works are quoted for comparison. The present results agree reasonably with the experimental results [2, 5].

Table 1. Calculated lattice parameters a (Å), c (Å), elastic constants C_{ij} (GPa), bulk moduli B (GPa), shear moduli G (GPa), Young's moduli E (GPa), and Poisson's ratio ν for Li_3P at T = 0 K.

Compound	a	c	C_{11}	C_{12}	C_{13}	C_{33}	C_{44}	B	G	E	ν
Li_3P	4.24	7.61	101.4	19.2	0.24	98.2	23.72	37.43	34.47	79.13	0.15
	4.23[a]	7.56[a]	-	-	-	-	-	-	-	-	-
	4.27[b]	7.59[b]	-	-	-	-	-	-	-	-	-
α-Li_3N	-	-	122.8[c]	24.6[c]	5.4[c]	129.5[c]	16.6[c]	-	-	-	-
β-Li_3N	-	-	131.8[c]	28.8[c]	8.7[c]	180.4[c]	37.1[c]	-	-	-	-

a: [5], b: [2], c: [21]

3.2. *Elastic properties*

The elastic constants define the properties of material that undergoes a stress, deforms and then returns to its original shape after stress ceases. These properties play an important part in providing valuable information about the binding characteristic between adjacent atomic planes, anisotropic character of binding and structural stability. The elastic moduli require the knowledge of the derivative of the energy as a function of the lattice strain. To study the elastic properties of Li_3P at T = 0 K and P = 0 GPa, the elastic constants C_{ij}, bulk modulus B, shear modulus G, Young's modulus E, and Poisson's ratio ν have been calculated for the first time. Theoretical details on elastic constants can be found elsewhere [22, 23]. The elastic constants of Li_3P calculated within GGA are reported in Table 1. Till date, no experimental or theoretical data for the elastic stiffness are available in the literature for comparison with our data. As a result our calculations can provide reference data for future investigations. However since Li_3N is also an ionic conductor like Li_3P, we have compared our calculated elastic constants with those of Li_3N [21].

The theoretical polycrystalline moduli for Li_3P may be computed from the set of independent elastic constants. Hill [24] proved that the upper and lower limits of the true polycrystalline constants are expressed from Voigt and Reuss equations. So the polycrystalline moduli are defined as the average values of the Voigt (B_V, G_V) and Reuss (B_R, G_R) moduli. According to Hill's observation, the value of bulk modulus (in GPa) $B = B_H = (B_V + B_R)/2$ (Hill's bulk modulus), where B_V and B_R are the Voigt's and the Reuss's bulk modulus respectively. The value of shear modulus $G = G_H = (G_V + G_R)/2$ (Hill's shear modulus), where G_V and G_R are the Voigt's and the Reuss's shear modulus respectively. The expressions for Voigt and Reuss moduli can be found in Ref. [21]. Using the two formulas: $E = 9BG/(3B + G)$ and $\nu = (3B - E)/6B$, the polycrystalline Young's modulus E (in GPa) and the Poisson's ratio ν are obtained and given in Table 1.

The condition for mechanical stability is that B, C_{11}-C_{12} and C_{44} are positive [25]. It is found that Li_3P is mechanically stable because B, C_{11}-C_{12} and C_{44} are positive. The ductitle-brittle nature of materials can be discussed in terms of elastic constants of the relevant material. If the Cauchy's pressure (C_{12}-C_{44}) is negative (positive), the material is

expected to be brittle (ductile) [26]. In the present case this value is negative and it indicate that Li_3P is brittle. Another index of ductility is Pugh's ratio [27] and a material behaves in a ductile manner, if $G/B < 0.5$, otherwise it should be brittle. The critical number which separates the ductile and brittle was found to be 0.57 [28]. Thus the value of 0.92 for Li_3P thus indicates its brittle behavior. The elastic anisotropy of crystal, defined by the ratio $A = 2C_{44}/(C_{11} - C_{12})$ [29], yields a value of 0.58 for A. The factor $A = 1$ represents complete isotropy, while value smaller or greater than this measures the degree of anisotropy. Therefore, Li_3P shows strong anisotropic behavior. The parameter $k_c/k_a = (C_{11}+C_{12}-2C_{13})/(C_{33}-C_{13})$ expresses the ratio between linear compressibility coefficients of hexagonal crystals [29]. From our data the value of k_c/k_a (= 1.6) indicates that the compressibility for Li_3P along c axis is greater than along a axis.

3.3. *Thermodynamic properties*

The investigation of thermodynamic properties under high temperature and high pressure requires the application of quasi-harmonic Debye approximation [15]. The thermodynamic properties of Li_3P have been investigated by using this model and for this we first derive E-V data obtained from Birch-Murnaghan equation of state [20] using zero temperature and zero pressure equilibrium values, E_0, V_0, B_0, based on DFT method. Then in order to get different thermodynamic properties at finite-temperature and finite-pressure, we apply the quasi-harmonic Debye model, in which the non-equilibrium Gibbs function $G^*(V; P, T)$ can be written in the form [15]:

$$G^*(V;P,T) = E(V) + PV + A_{vib}[\Theta(V);T] \tag{1}$$

where $E(V)$ is the total energy per unit cell, PV corresponds to the constant hydrostatic pressure condition, $\Theta(V)$ is the Debye temperature, and A_{vib} is the vibrational term, which can be written using the Debye model of the phonon density of states as [15]:

$$A_{vib}(\Theta;T) = nkT\left[\frac{9}{8}\frac{\Theta}{T} + 3\ln\left(1 - \exp\left(-\frac{\Theta}{T}\right)\right) - D(\Theta/T)\right] \tag{2}$$

where n is the number of atoms per formula unit, $D(\Theta/T)$ represents the Debye integral.

The non-equilibrium Gibbs function $G^*(V; P, T)$ can be minimized with respect to volume V to obtain the thermal equation of state $V(P, T)$ and the chemical potential $G(P, T)$ of the corresponding phase. Other macroscopic properties can also be derived as a function of P and T from standard thermodynamic relations [15]. Here we computed the bulk modulus, specific heats, Debye temperature and volume thermal expansion coefficient at different temperatures and pressures.

Fig. 1 shows the temperature and pressure dependent of bulk modulus B and Debye temperature for Li_3P. It is seen that bulk modulus and Debye temperature decreases smoothly with increasing temperature. Inset shows the pressure dependent of bulk

modulus and Debye temperature at 300 K. We see that B and Debye temperature both decreases slightly with increasing temperature.

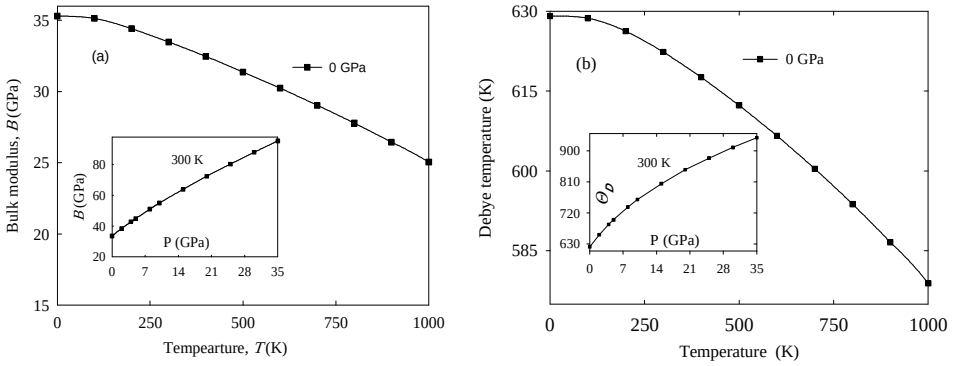

Fig. 1. The temperature dependence of (a) bulk modulus and (b) Debye temperature of Li_3P at $P = 0$ GPa. The insets to the figure show the pressure dependence of B and Θ_D, respectively at 300 K.

The thermal effect on the heat capacities C_V, C_P of Li_3P are shown in Fig. 2 (a, b). At high temperature ($T > 400$ K), the constant volume heat capacity C_V tends to the Dulong and Petit limit of $C_V = 3nNk_B = 99.74$ J/mol.K. At sufficiently low temperature, C_V is proportional to T^3. For a given temperature, C_V decreases with increasing pressure. The difference between C_P and C_V for Li_3P is given by $C_P - C_V = \alpha^2(T)\, BTV$, which is due to the thermal expansion caused by anharmonicity effects. These results show the fact that the interactions between ions in Li_3P have great effect on heat capacities especially at low temperatures. There is no theoretical or experimental value of specific heat capacities of Li_3P for comparison with the present calculated results.

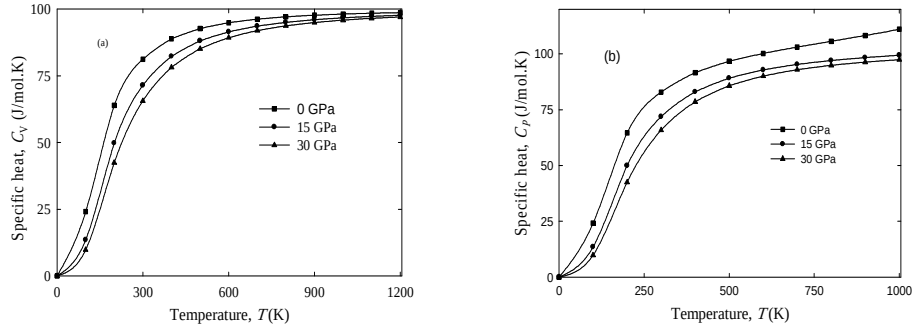

Fig. 2. The temperature dependence of specific heat at (a) constant-volume C_V and (b) constant-pressure C_P of Li_3P.

The volume thermal expansion coefficient, α reflects the temperature dependence of volume at constant pressure: $\alpha = \frac{1}{V}\left(\frac{dV}{dT}\right)_P$. The temperature dependence of α at zero pressure is displayed in Fig. 3 (a). The thermal expansion coefficient of Li_3P increases as the temperature increases. At a given temperature, α decreases drastically with the increase of pressure. Fig. 3 (b) shows the pressure dependence of thermal expansion coefficient at 300 K. It is well known that temperature and pressure effects on the volume are opposite. The increase in temperature can cause volume expansion and increase in pressure can suppress this effect. At high temperatures and high pressures, the thermal expansion would converge to a constant value. At a given pressure, α increases sharply with the increase of temperature up to 300K. When T = 300 K, α gradually approaches a linear increase with enhanced temperature and the propensity of increment becomes moderate, which means that the temperature dependence of α is smaller at higher temperature.

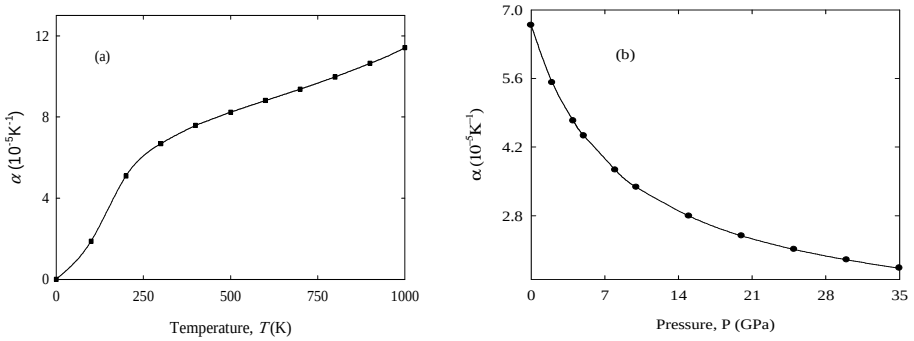

Fig. 3. The volume thermal expansion coefficient α of Li_3P as a function of (a) temperature and (b) pressure at 300K.

3.3. *Optical Properties*

The imaginary part of the dielectric function $\varepsilon_2(\omega)$ is calculated using the expression given in Ref. [11]. The real part $\varepsilon_1(\omega)$ of the dielectric function can be derived from the imaginary part using the Kramers–Kronig relation. From the real and imaginary parts of the dielectric function one can calculate the refractive index, reflectivity and electron energy loss spectra using the expressions given in Ref. [11]. The imaginary part $\varepsilon_2(\omega)$ is obtained from the momentum matrix elements between the occupied and the unoccupied electronic states and calculated directly using [11]:

$$\varepsilon_2(\omega) = (2e^2\pi/\Omega\varepsilon_0)\sum_{k,v,c}|\psi_k^c|\boldsymbol{u}.\boldsymbol{r}|\psi_k^v|^2\delta(E_k^c - E_k^v - E) \quad (3)$$

where $\boldsymbol{u}$ is the vector defining the polarization of the incident electric field, ω is the light frequency, e is the electronic charge and ψ_k^c and ψ_k^v are the conduction and valence band wave functions at k, respectively.

The optical functions of Li_3P have been calculated for photon energies up to 25 eV for polarization vectors [100] and [001] and only spectra for [100] are shown in Fig. 4. We have used a 0.5 eV Gaussain smearing for all calculations. The imaginary and real parts of the dielectric function are displayed in Fig. 4 (a). From Fig. 4 (a) it is found that the real part of the dielectric function vanishes at 13.4 eV. This value corresponds to the energy at which the reflectivity exhibit sharp peak shown in Fig 4 (e). The refractive index and extinction coefficient are illustrated in Fig. 4 (b). The static refractive index is found to have the value 2.76. The calculated optical conductivity at T = 0 K and P = 0 GPa is presented in Fig. 4 (c). The optical conductivity has a number of maxima and minima within the energy range studied. The absorption spectra is depicted in Fig. 4 (d) and it observed that absorption is maximum (23%) around 6 eV energy region.

Fig. 4 (e) shows the reflectivity spectra as a function of photon energy and it is found that a large reflectivity is obtained between 7 to 13.4 eV. This large reflectivity implies that Li_3P material would be a good reflector material in the ultraviolet region. The electron energy loss function describes the energy loss of a fast electron traversing in a material. The peaks in this spectrum represent the characteristic associated with the plasma resonance and the corresponding frequency is the so called plasma frequency ω_p. The peaks of energy loss correspond to the trailing edges in the reflectivity spectra, for instance, the prominent peaks of loss are situated at energies corresponding to the abrupt reduction of reflectivity. From Fig. 4 (f) it seen that the plasma frequency for Li_3P is 13.4 eV.

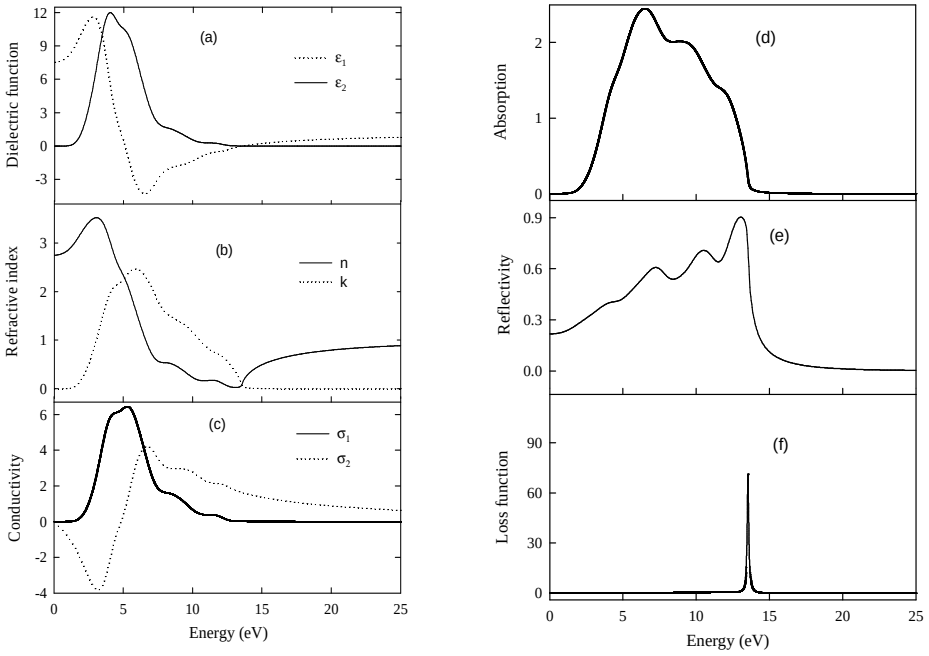

Fig. 4. Energy dependent (a) dielectric function, (b) refractive index and extinction coefficient, (c) conductivity, (d) absorption, (e) reflectivity, and (f) loss function of Li_3P along [100] direction.

4. Conclusion

First-principles calculations based on DFT have been used to study the elastic, thermodynamic and optical properties of Li_3P. The material is elastically anisotropic and shows brittle behavior. The finite-temperature ($\leq$ 1000 K) and finite-pressure ($\leq$ 35 GPa) thermodynamic properties, *e.g.* bulk modulus, Debye temperature, specific heats, and thermal expansion coefficient are all obtained through the quasi-harmonic Debye model, which considers the vibrational contribution, and the results are analysed. The variation of Θ_D with temperature and pressure reveals the changeable vibration frequency of the particles in Li_3P. The heat capacities increase with increasing temperature, which shows that phonon thermal softening occurs when the temperature increases. From the analysis of optical functions for the polarization vectors [100], it is found that the reflectivity is high in the ultraviolet region and it implies that Li_3P can be used as a coating material.

Reference

1. G. Nazri, Solid State Ionics **34**, 97 (1989). http://dx.doi.org/10.1016/0167-2738(89)90438-4
2. G. Nazri, Mater. Res. Soc. Symp. Pruc. **135**, 117 (1989). http://dx.doi.org/10.1557/PROC-135-117
3. G. Brauer and E. Zintl, Z. Phys. Chem. [Abt. B] **37**, 323 (1937).
4. Y. Dong. and F. J. DiSalvo, Acta Cryst. E **61**, i223 (2005). http://dx.doi.org/10.1107/S1600536805031168
5. Y. Dong. and F. J. DiSalvo, Acta Cryst. E **63**, i97 (2007). http://dx.doi.org/10.1107/S1600536807008422
6. C. Julien and G. A. Nazri, Solid State Batteries, Materials Design and Optimization (Kluwer Academic Publishers, 1994). http://dx.doi.org/10.1007/978-1-4615-2704-6
7. S. Suzuki, H. Fujita, Y. Asami, F. Homma and Y. Sato, New Mat. New Process **3**, 264 (1985).
8. P. E. Harvey, *In*: Proc. 4th International Meeting on Lithium Batteries, Vancouver, B.C. Canada, May 24-27, 1988.
9. Mat. Res. Soc. Symp. Proc. Vol. **135** (1989) Materials Research Society for Discussion of glassy electrolytes.
10. G. A. Nazri, R. A. Conell, and C. Julien, Solid State Ionics **86-87 (Part 1)**, 99 (1996). http://dx.doi.org/10.1016/0167-2738(96)00099-9
11. S. J. Clark, M. D. Segall, M. J. Probert, C. J. Pickard, P. J. Hasnip, and M. C. Payne, Z. Kristallogr. **220**, 567 (2005). http://dx.doi.org/10.1524/zkri.220.5.567.65075
12. J. P. Perdew, K. Burke, and M. Ernzerhof, Phys. Rev. Lett. **77**, 3865 (1996). http://dx.doi.org/10.1103/PhysRevLett.77.3865
13. D. Vanderbilt, Phys. Rev. B **41**, 7892 (1990). http://dx.doi.org/10.1103/PhysRevB.41.7892
14. H. J. Monkhorst and J. D. Pack, Phys. Rev. B **13**, 5188 (1976). http://dx.doi.org/10.1103/PhysRevB.13.5188
15. M. A. Blanco, E. Francisco, and V. Luaña, Comput. Phys. Comm. **158**, 57 (2004). http://dx.doi.org/10.1016/j.comphy.2003.12.001
16. M. A. Blanco, A. M. Penda´s, E. Francisco, J. M. Recio, R. Franco, J .Mol .Struct. Theochem. **368**, 245 (1996). http://dx.doi.org/10.1016/S0166-1280(96)90571-0
17. M. Flórez, J. M. Recio, E. Francisco, M. A. Blanco, A. M. Pendás, Phys. Rev. B **66**, 144112 (2002). http://dx.doi.org/10.1103/PhysRevB.66.144112
18. E. Francisco, J. M. Recio, M. A. Blanco, and A. M. Pendás, J. Phys. Chem. **102**, 1595 (1998). http://dx.doi.org/10.1021/jp972516j
19. E. Francisco, M. A. Blanco, and G. Sanjurjo, Phys. Rev. B **63**, 049107 (2001). http://dx.doi.org/10.1103/PhysRevB.63.094107

20. F. Birch, J. Geophy. Res. **83**, 1257 (1978). http://dx.doi.org/10.1029/JB083iB03p01257
21. M. A. Hossain, A. K. M. A. Islam, and F. N. Islam, J. Sci. Res. **1** (2), 182 (2009). DOI: 103329/jsr.v1i2.1763
22. L. Fast, J. M. Wills, B. Johansson, and O. Eriksson, Phys. Rev. B **51**, 17431 (1995). http://dx.doi.org/10.1103/PhysRevB.51.17431
23. S. Q. Wang and H. Ye, J. Phys.: Condens. Matter **15**, 5307 (2003). http://dx.doi.org/10.1088/0953-8984/15/30/312
24. R. Hill, Proc. Phys. Soc. London A **65**, 349 (1952). http://dx.doi.org/10.1088/0370-1298/65/5/307
25. D. C. Wallace, Thermodynamics of Crystals (Wiley, New York, 1972).
26. D. Pettifor. Mater. Sci. Technol. **8**, 345 (1992). http://dx.doi.org/10.1179/026708392790170801
27. S. F. Pugh, Philos. Mag. **45**, 823 (1954).
28. V. Kanchana and S. Ram, Intermetallics **23**, 39 (2012). http://dx.doi.org/10.1016/j.intermet.2011.12.014
29. C. M. Zener, Elasticity, Anelasticity of metals (University of Chicago Press, Chicago, 1948).